SUPPORTING INFORMATION
Determining the Mg^{2+} Stoichiometry for Folding an RNA Metal Ion Core

Rhiju Das, Kevin J. Travers, Yu Bai, Daniel Herschlag
Department of Physics, Stanford University, Stanford, California 94305
Department of Biochemistry, Stanford University, Stanford, California 94305

The Supporting Information includes descriptions of the hydroxyl radical footprinting, atomic emission spectroscopy, and Mg^{2+} indicator fluorescence titration techniques. Supporting Figures S1-S5 support points made in main text and include radical cleavage profiles for discussed RNA states; Hill fits for separate residues in 2 M NaCl and 2 M KCl backgrounds; AES measurements on control DNA duplexes; and fits of data to models with and without a two-metal-ion core.

Supporting Methods

RNA and DNA preparation

Wild type and A-bulge/U P4-P6 RNA constructs were prepared by *in vitro* transcription from PCR-generated DNA templates using T7 RNA polymerase.[1] The sequence changes in the A-bulge/U mutant are A183U, A184U, A186U, A187U, and G188U.[2]

RNA stocks used for fluorescent indicator dye and atomic emission spectroscopy (AES) experiments were prepared by addition of 50 mM Na-EDTA to quench transcription, precipitation with ethanol and sodium acetate (in some cases, an ammonium acetate/ethanol precipitation was carried out first), extraction with one volume of phenol, extraction with one volume of chloroform, and at least five buffer exchange steps with Microcon YM-50 concentrators (Millipore, MA) into a dialysis buffer of 2 M NaCl, 50 mM sodium 3-(N-morpholino)ethanesulfonic acid (Na-MES), pH 6.0, (fluorescent dye experiments) or 50 mM sodium 3-(N-morpholino)propanesulfonic acid (MOPS), pH 7.0, with 1 mM EDTA (AES experiments). Flowthrough buffer from the final exchange step was tested and shown to be free of nucleotides (less than one hundredth of the absorbance of the RNA stock at 260 nm). Residual EDTA was shown to be less than 0.01 mol/ mol RNA by control Mg^{2+} titrations with the flowthrough buffer in place of RNA samples in fluorescent dye experiments (see below). RNA stock concentrations were determined by UV absorbance and verified by atomic emission spectroscopy of phosphorus (see below). These RNA preparations were estimated to have less than 10% contamination with RNA fragments of other lengths, based on comparison to gel-purified RNAs on denaturing polyacrylamide gels stained with Stains-All (Sigma).*

For AES experiments, a second preparation of RNA was gel purified prior to the dialysis against Mg^{2+} stocks. The *in vitro* transcription reactions for this RNA were precipitated using ammonium acetate and 100% ethanol, resuspended in 10 mM Tris-HCl, pH 8.0, with 1 mM EDTA (TE), and run on 6% polyacrylamide gels containing 7.5 M urea. Gel slices containing RNA were cut from the gel, crushed, and put through three rounds of freezing and thawing. The RNA was eluted by soaking the gel pieces in TE, and recovered by precipitation with sodium acetate and ethanol.

Samples of a 24 base-pair DNA duplex were assembled from chemically synthesized oligonucleotides (Qiagen Operon Inc., CA) with sequence GGTGACGAGTGAGCTACTGGGCGG and its reverse complement. Oligonucleotides were purified by ion-exchange HPLC chromatography (Dionex, CA), desalted with C18 Sep-Pak cartridges (Waters, MA), dried to solid pellets, and resuspended in doubly distilled water. Equimolar (determined by absorbance at 260 nm) complementary strands were annealed in 50 mM Na-MOPS, pH 7.0, before buffer exchange for atomic absorbance measurements (see below).

Hydroxyl radical footprinting

Constructs were radiolabeled at the 5´-end with γ–^{32}P-ATP using T4 polynucleotide kinase or at the 3´-end with α–^{32}P-dATP using Klenow Exo$^-$ DNA polymerase and a 26 nucleotide DNA splint[3], purified by denaturing polyacrylamide gel electrophoresis, and buffer-exchanged into doubly deionized water by gel filtration in P30 Microspin columns (Bio-Rad, CA). Radiolabeled RNA samples (30k-50k cpm) were incubated at 25 ºC for 10 min with 50 mM Na-MOPS, pH 7.0; 0-50 mM $MgCl_2$; and 2 M NaCl, 2 M KCl, or no added salt. Hydroxyl radical cleavage was initiated by the addition of freshly prepared Fenton reagent at a final concentration of 0.1 mM $Fe(NH_4)_2(SO_4)_2$,

* Gel-purified RNA stocks could not be used in indicator dye experiments; such samples produced quenching and time-dependent changes in the dye signal, presumably due to residual acrylamide or polyacrylamide pieces that remained even after filtration through 0.2 μm membranes. Mg^{2+}-counting measurements with atomic emission spectroscopy (see below) carried out with RNAs prepared as described above were indistinguishable from those carried out with gel-purified RNA.

0.125 mM EDTA, and 10 mM sodium ascorbate. After incubation at 25 °C for 60 minutes, the reactions were stopped with a half volume of a quench solution (100 mM thiourea, 0.1% xylene cyanol, 0.1% bromophenol blue in formamide). The reaction products were separated by polyacrylamide gel electrophoresis, and visualized by phosphor storage imaging. Gel autoradiograms were quantitated with single nucleotide resolution using the SAFA program,[4] and the resulting data were normalized to correct for small lane loading variations.[4,5] Under the reaction condition, hydroxyl radical cleavage is limited to one cut per RNA or less; such "single-hit kinetics" reaction conditions were verified by checking that the intensity of the uncleaved band is reduced by less than 15% compared to the band in a sample without Fenton reagent.

For Hill fits of individual residues over a Mg^{2+} titration, the relative protection for a residue *j* at Mg^{2+} concentration *i* is calculated as:

$$\text{Relative Protection} = f_j^i = \frac{A_j^i - A_j^{unfold}}{A_j^{fold} - A_j^{unfoldi}} \quad \text{(S1)}$$

These values were fit to the Hill equation:

$$f_j^i = \frac{([Mg^{2+}]_i / K)^n}{1 + ([Mg^{2+}]_i / K)^n} \quad \text{(S2)}$$

Two data sets with 2 M NaCl and one data set with 2 M KCl were collected; global Hill fits to all residues with Mg^{2+}-dependent protections yielded small statistical errors in the Hill parameters (standard errors of ±0.008 mM for the folding midpoint; ±0.06 for the Hill coefficient, estimated by bootstrapping[6]). However, the uncertainty in the fitting parameters is dominated by another source of error: an uncertainty of approximately ±0.025 mM in the EDTA concentration introduced with the Fenton reagent. Assuming that the free Mg^{2+} concentration has a corresponding uncertainty, systematic errors of ±0.025 mM in the folding midpoint and ±0.1 in the Hill coefficient are estimated for these measurements. Note that these values are appropriate standard errors for the Hill parameters *averaged* over all probed residues; errors on Hill parameters for individual residues are larger, as shown in Figs. S2 and S3.

Mg^{2+} counting with atomic emission spectroscopy

Microcon YM-50 filters and YM-30 filters were used to dialyze RNA and DNA samples, respectively, into the appropriate Mg^{2+}-containing buffers (50 mM Na-MOPS, pH 7.0, 2 M NaCl, and 0-5 mM $MgCl_2$). A total of four dilutions and centrifugation steps were performed for each sample to ensure that equilibrium was reached. Aliquots of eluted nucleic acid and flow-through were then diluted into 5 mL ultrapure water (Barnstead, IA). Concentrations of phosphorus, sodium, magnesium, and sulfur were measured simultaneously from these dilute samples using an IRIS Advantage/1000 Radial ICAP Spectrometer (Thermo Jarrell Ash, MA) and compared to standards with known amounts of each element. Controls were carried out to ensure that there was no interference between the measurements of the four elements analyzed here (P, Na, Mg, and S) and that the presence of RNA or DNA did not affect any of the measured elemental concentrations. The number of metal ions associated with a nucleic acid sample was calculated as the difference in magnesium concentration between the nucleic-acid-containing sample and its corresponding flow-through, divided by the nucleic acid concentration determined by the AES phosphorus measurement. Instrument errors were estimated from variances of measurements made on standard curves for each element analyzed. The values presented in the text are the average of the measurements at each Mg^{2+} concentration, weighted by the inverse-square instrument errors, and the reported uncertainties are ± one standard error, based on the propagated instrument error.

The number of ions associated with a polyelectrolyte can become dependent on the concentration of polyelectrolytes at high concentrations if aggregation or intermolecular ordering occurs. To test this possibility, two to four measurements were made at each Mg^{2+} concentration, at nucleic acid concentrations ranging from 120 to 400 μM (RNA) and from 300 to 700 μM (DNA); measurements at different nucleic acid concentrations agreed within instrument errors. Additionally, no significant differences were observed with RNA that was gel purified compared to non-gel-purified RNA.

Mg^{2+} counting with a fluorescent indicator dye

Measurements with the Mg^{2+}-dependent indicator dye 8-hydroxyquinoline-5-sulfonic acid (HQS) were carried out on a SPEX Fluorolog fluorometer (Horiba Jobin Yvon, NJ) with excitation wavelength 400 nm (4 nm bandpass) and with emission wavelength 550 nm (4 nm bandpass). Unlike the footprinting experiments and AES experiments at pH 7.0, the HQS experiments were carried out at pH 6.0 to prevent significant perturbation of the free Mg^{2+} concentration by the HQS dye (see below); the effect of the different pH on Mg^{2+} association to the RNA was found to be negligible, based on indistinguishable values for AES measurements on the wild type RNA at 1 mM $MgCl_2$, 2 M NaCl, 50 mM Na-MES pH 6.0, and at 1 mM $MgCl_2$, 2 M NaCl, 50 mM Na-MOPS pH 7.0.

In a typical HQS experiment, samples were prepared by mixing 23 μL of a dye stock (0.2 mM HQS, 2 M NaCl, 50 mM Na-MES, pH 6.0) with 23 μL of the dialysis buffer (2 M NaCl, 50 mM Na-MES, pH 6.0) or of the RNA stock (0.12–0.8 mM RNA in the same buffer) and pipetted into a fluorescence cuvette. Titrations were carried out by

manually pipetting 1 μL aliquots of a Mg^{2+} stock (8 mM $MgCl_2$, 0.1 mM HQS, 2 M NaCl, 50 mM Na-MES, pH 6.0) into the cuvette, followed by stirring with the pipette tip. Fluorescence measurements (1 second exposures) did not change detectably with increased exposure to photoexcitation (up to one minute) or further sample mixing, indicating that photobleaching of the HQS dye can be neglected. Approximately 1-2 minutes separated each of the 25 Mg^{2+} additions; waiting up to ten minutes between measurements produced no detectable change in fluorescence, consistent with fast equilibration of the samples during the titration.

The standard curve relating HQS fluorescence to the free Mg^{2+} concentration was obtained from the control measurements without RNA. The curve at 2 M NaCl, 50 mM Na-MES, pH 6.0, was indistinguishable from a standard binding isotherm with apparent dissociation constant $K_d = 20$ mM; as a consistency check, analogous curves taken at 50 mM Na-MES, pH 6.0 (no added NaCl) gave a dissociation constant of 10 mM, consistent with the tabulated value of 10 mM for Mg^{2+}-HQS association extrapolated to pH 6.0.[7] The weak affinity of the indicator dye for Mg^{2+} ensures that the free Mg^{2+} concentration is perturbed by no more than ~0.5% by the dye in these experiments; measurements with 2-4 fold lower HQS concentrations also gave indistinguishable results.

The number of Mg^{2+} ions associated with the RNA at each point in the titration was determined by subtracting the free Mg^{2+} concentration (inferred from the HQS fluorescence and standard curve) from the known added Mg^{2+} concentration, and then dividing this value by the RNA concentration. Measurements with RNA concentrations different by four fold gave consistent results. Data presented in the main text are averages of four replicate measurements each of the wild type and A-bulge/U constructs from three independently transcribed and purified RNA stocks. The presented errors were estimated from the variance between replicates. Unlike the AES measurements, the errors in the HQS measurements at different Mg^{2+} concentrations are not independent; small pipetting errors early in the titration affect measurements at later points in the titration. As a consequence, the number of Mg^{2+} associated with the RNA in individual replicate experiments is systematically lower or systematically higher than the final average between replicates; the apparent systematic difference between HQS and AES measurements on the mutant RNA shown in Figure 2a of the main text is consistent with the HQS measurement error.

Models with and without a two-metal-ion core

The Hill analysis of footprinting isotherms presented in the main text supports a model where the P4-P6 state with a folded metal ion core is associated with two more metal ions than the unfolded state. The simple Hill analysis, in the absence of metal ion counting, is consistent with a two-metal-ion core (Model 1), but it is also consistent with a model in which the metal ion core is associated with three or more ions (Model 2). The latter model requires, however, that at least one Mg^{2+} be pre-associated to the RNA at Mg^{2+} concentrations well below the range where the folding transition is observed (0.2–1 mM Mg^{2+}). We have tested these two models (Schemes S1 and S2) by comparing our experimental measurements to the models' predictions for both the folding equilibrium and for Mg^{2+}-association to the wild type P4-P6 RNA.

Scheme S1. Model 1: Metal ion core folded state (F) has a minimum of two metal ions.

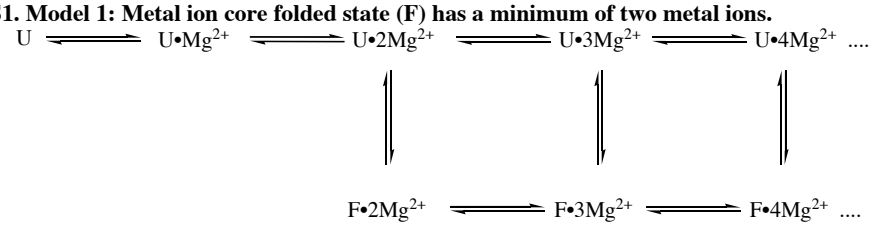

Scheme S2. Model 2: Metal ion core folded state (F) has more than two metal ions.

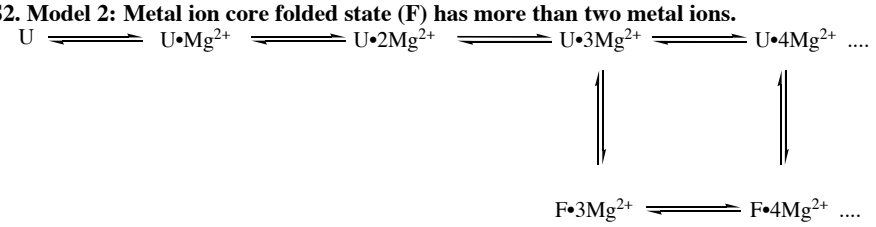

Schemes S1 and S2 separate the unfolded and folded states into sub-states according to how many Mg^{2+} ions are thermodynamically associated (not necessarily site-bound) to the sub-state. A sub-state that is associated with n Mg^{2+} ions has a weight proportional to $[Mg^{2+}]^n$ (see, e.g., refs[8-10]), and the coefficients of proportionality a_n^U and a_n^F are constrained by folding equilibrium and Mg^{2+}-association data, as follows. The fraction of the RNA in the folded state is given by:

$$f_F = \frac{a_2^F[Mg^{2+}]^2 + a_3^F[Mg^{2+}]^3 + \ldots}{Z}, \qquad \text{(S3)}$$

where Z is the partition function, the sum of the weights of all the states:

$$\begin{aligned} Z &= Z_U + Z_F \\ Z_U &= 1 + a_1^U[Mg^{2+}] + a_2^U[Mg^{2+}]^2 + a_3^U[Mg^{2+}]^3 + \ldots \\ Z_F &= a_2^F[Mg^{2+}]^2 + a_3^F[Mg^{2+}]^3 + \ldots \end{aligned} \qquad \text{(S4)}$$

Note that in the case where $Z_F \propto Z_U^n$, the Hill equation (S2) holds by definition, as was assumed in the main text. Our aim here is to test the general case where the weights of the sub-states in Schemes 1 and 2 are not necessarily forced to satisfy this proportionality constraint.

The number of Mg^{2+} ions associated with the RNA is:

$$\text{number } Mg^{2+} \text{ bound} = \frac{a_1^U[Mg^{2+}] + 2(a_2^U + a_2^F)[Mg^{2+}]^2 + 3(a_3^U + a_3^F)[Mg^{2+}]^3 + \ldots}{Z} \qquad \text{(S5)}$$

Expressions (S3)-(S5) hold for Model 1, with a minimal two-metal-ion core. For Model 2, which requires more than two metal ions to fold the core, we require $a_2^F = 0$. The data constrain coefficients a_n^U and a_n^F with n up to 4; higher order terms are not included since no more than 4 Mg^{2+} ions are associated with the RNA over the probed $MgCl_2$ concentrations. We fitted the footprinting data and AES measurements for the wild type P4-P6 RNA by χ^2 minimization with the Nelder-Mead algorithm in Matlab (MathWorks, Inc., MA), and the best-fit curves are shown in Figure S5. Model 1 (Scheme 1; two metal ion core) gives excellent fits to the data. In contrast, Model 2 (Scheme S2; more than two metal ions in core) gives predictions that deviate systematically from both the folding equilibrium and Mg^{2+}-association data sets.

Supporting References

(1) Milligan, J. F.; Uhlenbeck, O. C. *Methods Enzymol*. **1989,** *180*, 51-62.
(2) Takamoto, K.; Das, R.; He, Q.; Doniach, S.; Brenowitz, M.; Herschlag, D.; Chance, M. R. *J. Mol. Biol.* **2004,** *343*, 1195-206.
(3) Huang, Z.; Szostak, J. W. *Nucleic Acids Res.* **1996,** *24*, 4360-1.
(4) Das, R.; Laederach, A.; Pearlman, S. M.; Herschlag, D.; Altman, R. B. *RNA* **2005,** *11*, 344-54.
(5) Takamoto, K.; Chance, M. R.; Brenowitz, M. *Nucleic Acids Res.* **2004,** *32*, E119.
(6) Efron, B.; Tibshirani, R., *An introduction to the bootstrap*. Chapman Hall: New York, 1993.
(7) Bjerrum, K.; Schwarzenbach, G.; Sillen, L. G.; Anderegg, G.; Rasmussen, S. E., *Stability constants of metal-ion complexes, with solubility products of inorganic substances. Part 1: Organic ligands*. The Chemical Society: London, 1957.
(8) Bina-Stein, M.; Stein, A. *Biochemistry* **1976,** *15*, 3912-7.
(9) Leroy, J. L.; Gueron, M. *Biopolymers* **1977,** *16*, 2429-46.
(10) Misra, V. K.; Draper, D. E. *Biopolymers* **1998,** *48*, 113-35.

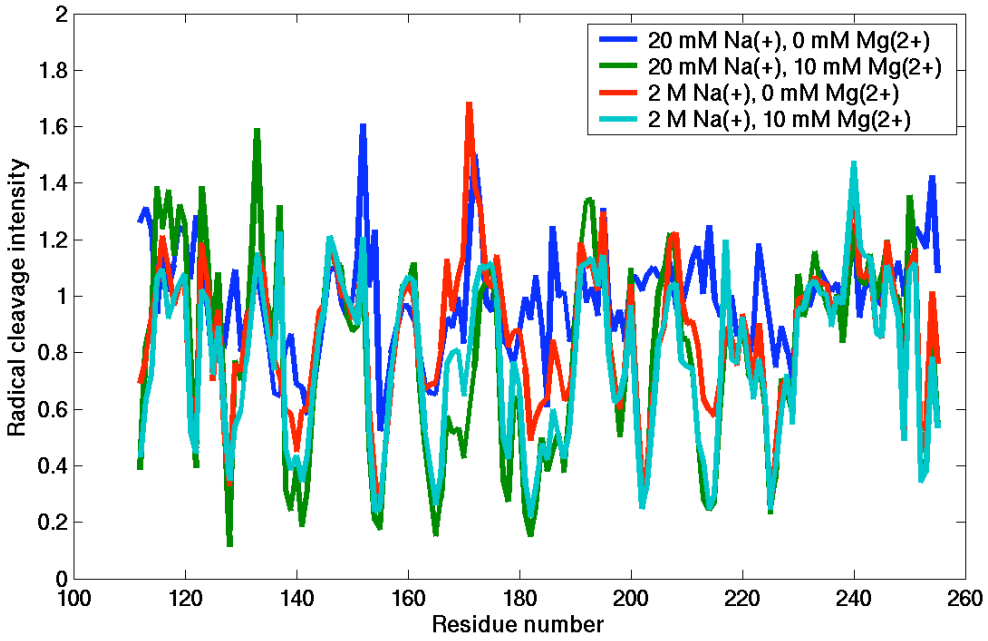

Figure S1. Hydroxyl radical cleavage profiles of the states of the wild type P4-P6 RNA discussed in the text. Profiles have been normalized to residues whose reactivities appear invariant upon folding;[5] errors are ±0.1 or better at all residues, based on variance between footprinting experiments with 5´- and 3´- radiolabeled RNA. The native state in 20 mM Na^+, 10 mM Mg^{2+} (green) shows distinct protections relative to an unfolded state without tertiary contacts in 20 mM Na^+, no Mg^{2+} (blue).[2] The partially folded state in high sodium, 2 M Na^+, no Mg^{2+} (red) shows many of the native protections except in regions that form the "magnesium core" of P5abc (135–145; 160–190) and its docking site in P4 (210–215). These regions display a protection pattern consistent with the native state upon the addition of Mg^{2+} (cyan). Small residual differences at 165–170 between Mg^{2+}-folded states at 20 mM Na^+ and 2 M Na^+ are reproducible and remain at the highest Mg^{2+} concentrations tested (50 mM $MgCl_2$); these differences may reflect a small structural difference in 2 M NaCl, a more dynamic P5c stem in 2 M NaCl, and/or a difference in electrostatic potential affecting the approach of the negatively charged radical source $[Fe(II)•EDTA]^{2-}$.

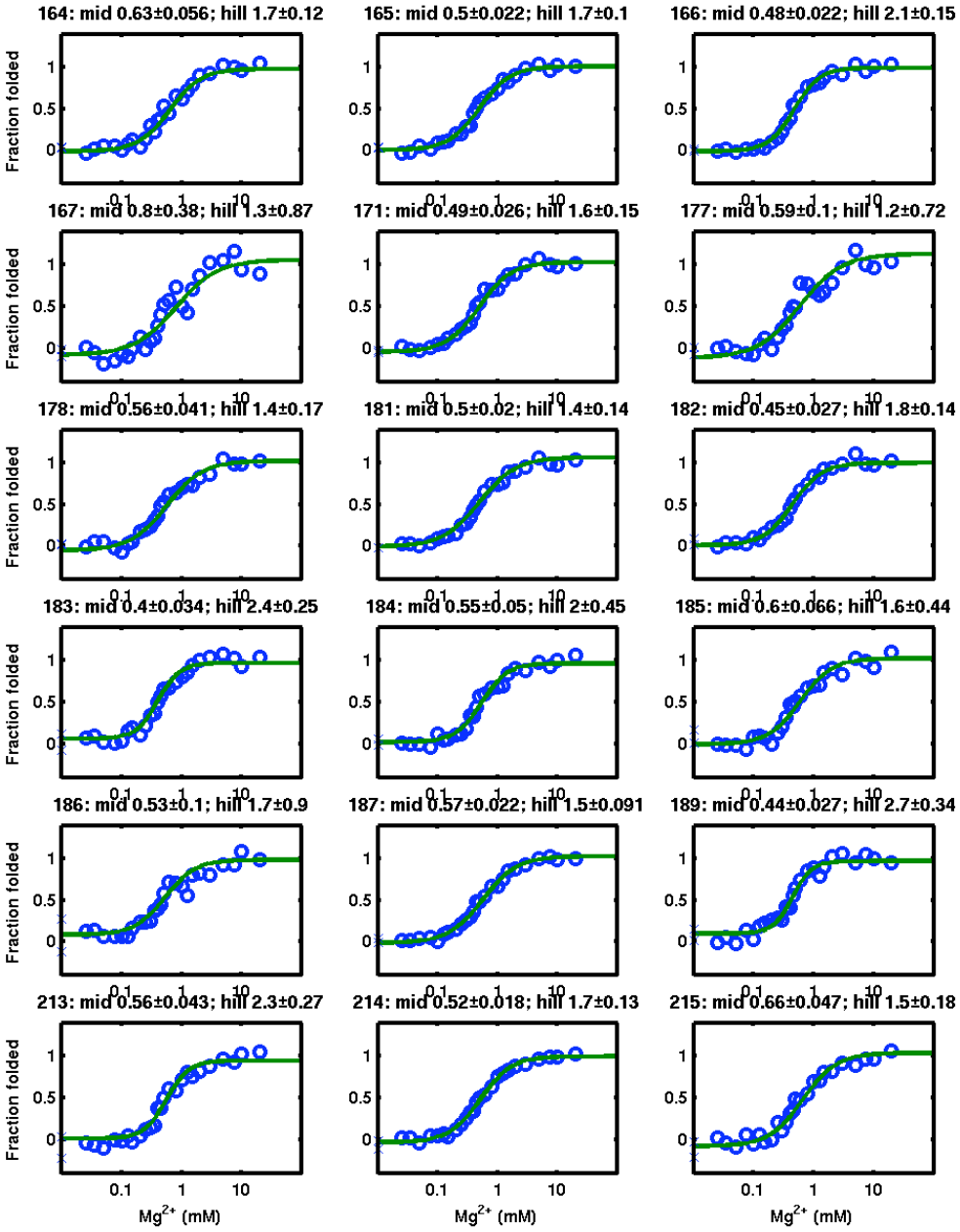

Figure S2. Folding behavior in a background of 2 M NaCl monitored at separate residues whose radical reactivity changes significantly (more than 30%) as a function of Mg^{2+} concentration. The data for each residue are fit separately to the Hill equation (green lines; see titles of individual plots); the fitted Hill parameters for each residue are consistent with an average folding midpoint of 0.52 mM and average Hill coefficient of 1.8.

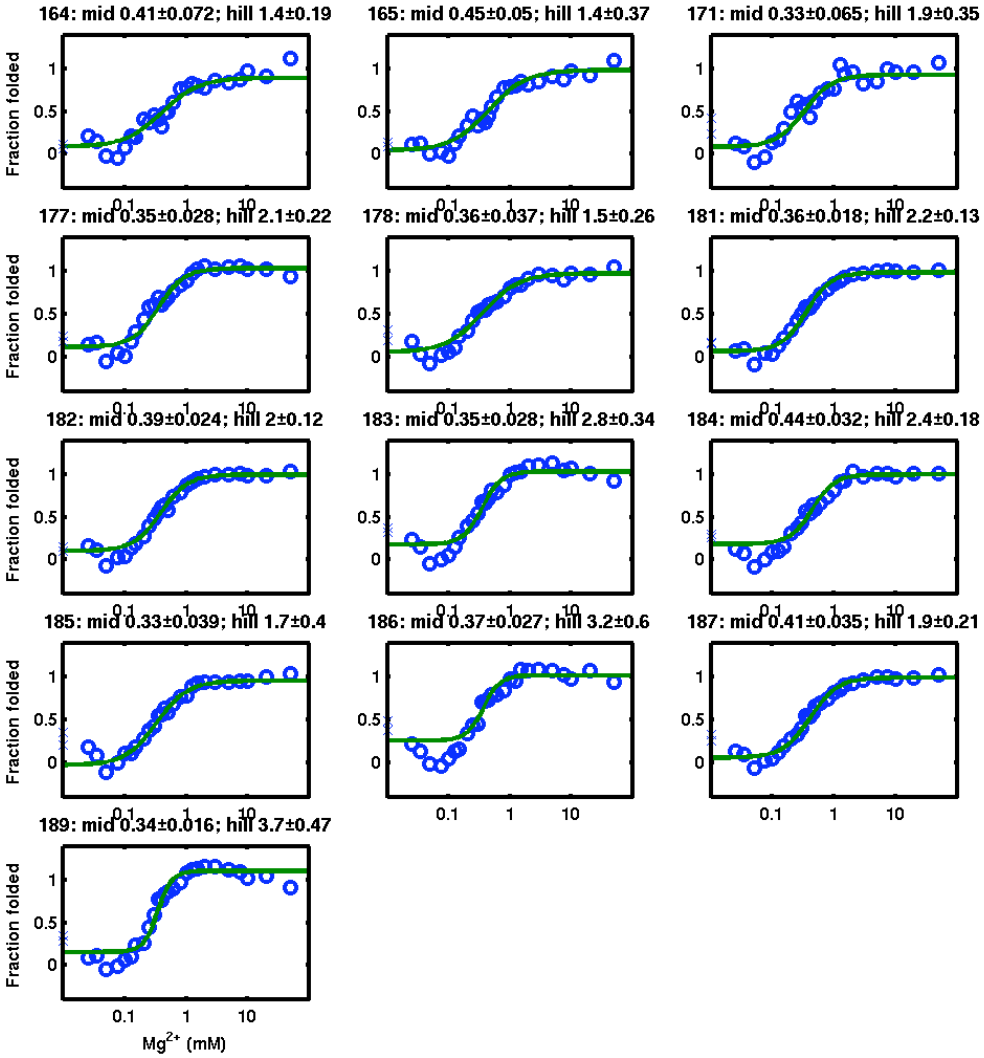

Figure S3. Mg^{2+}-dependent folding behavior in a background of 2 M KCl is similar to folding in a background on 2 M NaCl (see Figure S3 and Figure 1b in main text). The data for each residue are fit separately to the Hill equation (green lines; see titles of individual plots); the fitted Hill parameters for each residue are consistent with an average folding midpoint of 0.37 mM and average Hill coefficient of 2.0.

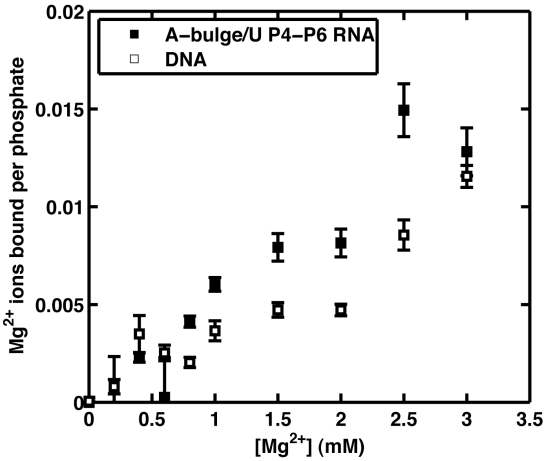

Figure S4. Atomic emission spectroscopy measurements for a 24 base-pair DNA duplex provide estimates of non-specific Mg^{2+} association to a nucleic acid in a 2 M NaCl background. The Mg^{2+} association with the DNA molecule (open squares), which is not expected to have specific metal ion binding sites, is compared to Mg^{2+} association with the metal-ion-core-less A-bulge/U P4-P6 RNA construct (solid squares). Because the molecules have different overall charges, the numbers of associated ions are normalized to the phosphate charge per molecule. The Mg^{2+} association behaviors are similar; a systematic ~30% difference is visible, possibly due to the different electrostatic potentials in the extended DNA molecule and the more globular P4-P6 RNA conformation.

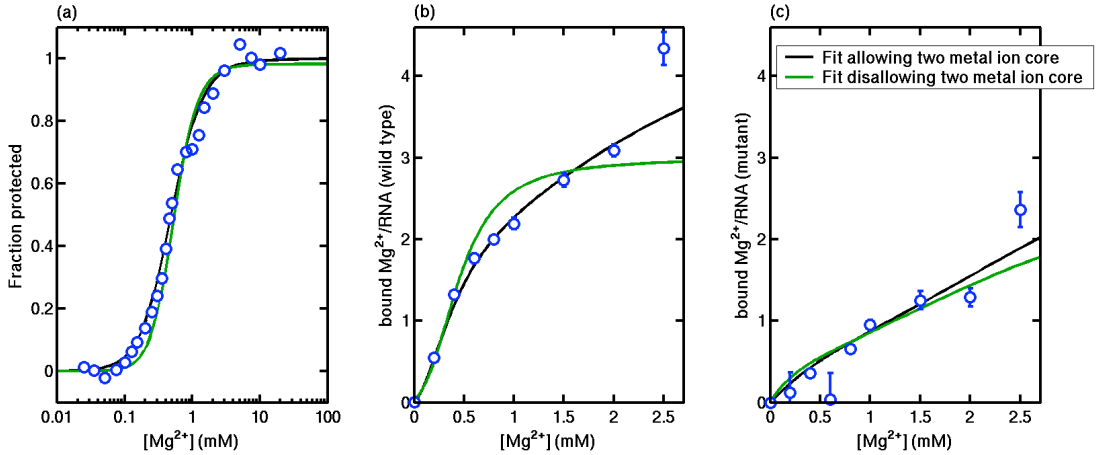

Figure S5. Folding equilibrium data from radical footprinting (a) and Mg^{2+}-association data from atomic emission spectroscopy (b) were fit to two models for the wild type P4-P6 RNA. The first model (black lines) allows the metal-ion-core-folded state to have two metal ions or more and faithfully reproduces both data sets. The second model (green) requires the metal-ion-core-folded state to have more than two metal ions. The folding equilibrium data ($n_{Hill} \sim 2$) constrains the Mg^{2+} uptake to be two ions upon folding. Thus, for the second model (a folded state with at least three Mg^{2+} ions) to hold, the at least one Mg^{2+} ion would need to be associated with the unfolded state at Mg^{2+} concentrations significantly lower than those at which folding occurs (0.2–1 mM). However, the Mg^{2+}-association data in (b) disfavor this possibility. As a result, the best-fit predictions from the second model fit neither the folding equilibrium nor the Mg^{2+}-association data well, strongly disfavoring this model that requires the metal-ion-core-folded state to have more than two Mg^{2+} ions. The Mg^{2+}-association data for the metal-ion-core-disrupted mutant are not necessary to make this conclusion, and these data (c) are fit well by both models under consideration.